Right anterior insula effective connectivity impairs intrinsic BOLD fluctuations in dorsal attention network in adolescents and young adults with borderline personality symptoms

Nathan T. Hall[1] and Michael N. Hallquist[1]

[1] Department of Psychology and Neuroscience, University of North Carolina at Chapel Hill

Disclosures. The authors have no financial interests to disclose.

Acknowledgments. This work was funded by the National Institutes of Mental Health (K01 MH097091 and R01 MH119399 to MNH). The funding agency had no role in the design and conduct of the study; the collection, management, analysis, and interpretation of the data; the preparation, review, and approval of the manuscript; or the decision to submit the manuscript for publication.

Corresponding author. Michael Hallquist, Department of Psychology and Neuroscience, University of North Carolina at Chapel Hill. 235 E. Cameron Avenue, Chapel Hill, NC 27599. michael.hallquist@unc.edu.

Abstract

Background: Borderline Personality Disorder (BPD) symptoms often emerge in adolescence. However, little is known about the functional organization of intrinsic brain networks in young people with BPD symptoms.

Methods: In this study we collected resting-state fMRI data in a sample of adolescents and young adults with (n_{BPD} = 40) and without BPD (n_{HC}= 42) symptoms. Using a detailed cortico-limbic parcellation coupled with graph theoretical analyses, we tested for group and age-related differences in regional functional and effective connectivity (FC, EC) and amplitude of low frequency fluctuations (ALFF). We conducted a series of analyses that progressed from global network properties to focal tests of EC amongst nodes in Salience (SN) and Dorsal Attention Networks (DAN).

Results: At the regional level, regularized regression analyses revealed a broad pattern of hyper-connectivity and heightened ALFF in R dorsal anterior insula (daIns), in addition to hypoconnectivity in R temporal-parietal junction (TPJ) and decreased ALFF in multiple DAN regions. Furthermore, analyses of EC amongst daIns, TPJ, and DAN revealed that in BPD participants daIns exerts a heightened influence on TPJ and DAN regions. Finally, multivariate mediation models indicated that lower DAN_{ALFF} was differentially predicted by EC from TPJ and daIns.

Conclusions: Our findings provide converging evidence that heightened EC from daIns impairs network-wide ALFF in DAN both directly and indirectly via impaired TPJ functioning. We interpret this pattern of findings in line with an “attentional hijacking” account of borderline personality.

Right anterior insula effective connectivity impairs intrinsic BOLD fluctuations in dorsal attention network in adolescents and young adults with borderline personality symptoms

Symptoms of Borderline Personality Disorder (BPD) such as emotion dysregulation and nonsuicidal self-injury typically emerge in adolescence (1,2). Although the maturation of circuits underlying emotion regulation and cognitive control is remarkable during this period (3), little is known about macroscale functional brain organization in young people with BPD symptoms. The current study investigated interactions among intrinsic connectivity networks in adolescents and young adults with BPD symptoms using three major BOLD indices of resting-state brain function: functional and effective connectivity (FC and EC, respectively) and regional amplitude of low-frequency fluctuations (ALFF; 4–6). Through a series of analyses that progress from broad network properties to focal tests of the relation between ALFF and EC in specific networks, we show that heightened resting-state effective connectivity of the R dorsal anterior insula (daIns) in BPD impairs ALFF in the Dorsal Attention Network (DAN).

Our study builds on evidence from developmental neuroscience that the organization of the brain into distinct networks (aka “modules”) is well-established by late childhood, though connectivity patterns amongst these networks undergoes a protracted refinement in adolescence (7–9). By late childhood, intrinsic networks have *segregated* (i.e., increased within-network connections), establishing the functional specializations of each network (9–11). However, during adolescence, functional *integration* among networks facilitates widespread communication via “connector hub” regions that serve as highways of between-network communication, which may underlie adolescence-related improvements in behavioral performance (8).

Crucially, in adolescence, the Salience Network (SN; 12,13) undergoes substantial changes in between-network connectivity compared to other intrinsic networks (8,14). SN is composed primarily of dorsal anterior cingulate (dACC) and aIns and plays a key role in detecting and orienting attention to stimuli that are behaviorally relevant or perceptually salient (12,15). A recent taxonomy of intrinsic networks expanded SN to include right temporal-parietal junction (TPJ) and inferior frontal gyrus (IFG) as well as numerous subcortical regions (16). SN is thought to organize dynamic switches among task-positive networks (DAN, Fronto-Parietal

Networks) and the task-negative Default Mode Networks (DMN; 15,17–19). In other words, SN monitors both internal and external events and triggers the appropriate networks to come online to implement either higher-order cognitive functions (DAN, FPN) or self-reflective internally directed thought (DMN). Within SN, the insula is a multimodal hub of cognitive-emotional functioning that receives sensory, cognitive, and homeostatic inputs; its integration of these signals facilitates flexible decision-making (13,20–22). More importantly, numerous studies of insula EC converge on its role as a central "outflow hub"; its widespread projections to cortex suggest a unique ability to control macroscale brain dynamics (18,19).

Given SN's involvement in a wide array of socio-cognitive and emotional processes and its protracted development in adolescence, it has become a key target in understanding the emergence of psychopathology (23–27). However, SN functioning in adolescents and young adults with BPD symptoms is poorly understood. Task-based fMRI studies of BPD have implicated a diverse set of regions involved in cognitive control, emotion regulation, and social cognition (28–32). However, few studies of intrinsic connectivity in adults with BPD have focused on SN (33–35). These studies have provided promising, though mixed, results regarding SN connectivity in borderline personality[1]. For example, two connectivity studies using ICA reported contradictory results: one found greater SN-DMN connectivity in BPD, while the other reported decreased SN-DMN connectivity (33,34).

This contradiction notwithstanding, there is good reason to believe that aberrant segregation and/or integration of DMN, SN, and task-positive networks may be associated with the expression of BPD symptoms. An influential "triple network model" of psychopathology argues that disrupted interactions among these networks likely contribute to the pathophysiology of numerous psychiatric disorders (23). This model posits that aberrant salience signals computed in aIns project to DMN and fronto-parietal regions, with major downstream effects on the cognitive processes implemented by these networks. For example, hyperactivity/connectivity of the aIns has been proposed to support heightened interoceptive prediction signals

[1] For a summary of findings from all published rsFC studies of adults with BPD we refer the interested reader to Table S1.

in anxiety (36), while hypoactivity of the aIns may underlie weakened salience mapping to social stimuli in autism (27,37).

Although SN likely plays an important role in psychopathology (38), the role of SN's connectivity with other networks and/or aberrant functioning of specific brain regions within SN remain topics of active inquiry in clinical studies. From the perspective of the triple network model, interpersonal hypersensitivity and volatile emotionality in BPD can be understood in terms of heightened salience mapping, with corresponding activity and connectivity of core SN regions. These salience signals would likely disrupt networks involved in planning and goal-directed behavior (FPN) and self-referential thought (DMN). Importantly, this model does not distinguish between task-positive networks involved in cognitive control and attentional control [FPN, DAN respectively; 38]. In a separate line of research, regions in SN have been shown to dynamically interact with parietal regions in DAN by generating attentional reorienting signals that interrupt transient attentional processing in DAN (40). However, aberrant communication between SN and DAN has received little attention in clinical neuroimaging studies.

Studies of SN in BPD have reported broad abnormalities, yet they have not clarified whether aberrant SN function is localized to specific regions, reflects interactions among SN regions, or may be a network-level phenomenon involving SN's coordination with other networks. Moreover, essentially no prior studies of BPD have characterized the functioning of intrinsic networks within a graph theoretical framework, the preferred analytic approach in network neuroscience (41,42). Graph theory represents networks in terms of regions ('nodes') and connections amongst regions ('edges') and offers a broad palette of metrics/analytic approaches that quantify an array of network properties. Importantly, these network properties can be conceptualized in terms of telescoping levels of analysis (43), from global (average connection strength across the entire network) to highly specific (edge characteristics between two nodes). Furthermore, while most connectivity studies in BPD focus on FC (undirected/correlational connectivity), modern EC models support inferences about the directionality of connectivity amongst regions (44–46). In a prior report, we investigated BPD-related differences in EC of amygdala subnuclei and targeted regions in mPFC (47), building on evidence of fronto-

limbic dysfunction in BPD (28,48,49). Here, we significantly broadened our scope to a whole-brain connectivity analysis, placing a particular emphasis on intrinsic activity and connectivity of SN and its constituent regions.

While connectivity analyses reveal features of the brain's functional network architecture, they provide less information about the magnitude of intrinsic activity. Markers of intrinsic activity provide information on the functional integrity of synchronized neural activity in a brain region. For example, FDG-PET studies have found a pattern of glucose hypometabolism in the medial PFC in BPD patients, suggesting abnormalities in the functioning of this region (50). In fMRI data, ALFF is a measure of the amplitude of low-frequency BOLD oscillations [0.01-0.1 Hz; 51], approximating the resting-state activity of a region (52). More specifically, basic studies of ALFF suggest a positive linear relationship between ALFF and glucose metabolism (53) and an inverse linear relationship between ALFF and GABA levels (54). Although ALFF provides an indirect index of regional intrinsic activity[2], to our knowledge no studies have focused on how connectivity between regions or networks may impair or bolster ALFF.

In a sample of adolescents and young adults with and without BPD symptoms, we examined whole-brain intrinsic connectivity using graph theoretical network measures and tested how connectivity patterns amongst these intrinsic networks are related to regional ALFF. As detailed below, our results suggest that in adolescents and young adults with BPD symptoms, the right dorsal aIns (daIns) is hyperactive (heightened ALFF) and exhibits a strengthened directed influence on DAN, which impairs network-level activity in DAN.

Materials and Methods

Participants

A thorough description of the current sample, including exclusion due to low rs-fMRI data quality is reported elsewhere (47; see Supplemental Materials). In short, we retained a final sample of 82 age- and sex-

[2] Throughout the rest of this paper, we use ALFF and "resting-state activity" interchangeably, though we encourage readers to keep in mind that this perhaps a rough equivalence.

matched adolescents and young adults (n_{BPD} = 40, mean age = 20.53, age range 13-30) with and without clinically heightened BPD symptoms. Detailed demographic information can be found in Table 1.

Procedure

Participants completed two semi-structured diagnostic interviews assessing psychopathology and personality disorder symptoms (55,56). Interviews were administered by research assistants trained and supervised by the senior author. Participants in the BPD group met diagnostic criteria for three or more of the DSM-IV-TR BPD symptoms (47,57). Exclusionary criteria included having a first-degree relative diagnosed with Bipolar I disorder or any psychotic disorder and a history of serious head injury or neurological disease. In addition, control participants had no history of psychiatric or substance abuse disorders.

Prior to the RS-fMRI session, participants completed a battery of self-report measures including the Borderline Personality Questionnaire (BPQ; 58). The BPQ is an 80-item self-report measure which measures the various BPD symptom dimensions based on the nine DSM criteria. Internal consistency among these scales was good to excellent in our sample (α_{BPQ} = 0.97, mean subscale α_{BPQ} = 0.86).

MR Data Acquisition

Data were acquired using a Siemens 3T Tim Trio scanner with a 32-channel head coil at the University of Pittsburgh Medical Center. We collected five minutes of resting-state fMRI data during which subjects were asked to keep their eyes open and relax, but not fall asleep. We used a simultaneous multi-slice echo-planar sequence sensitive to BOLD contrast with scanning parameters: TR = 1.0s, TE = 30ms, FoV = 220 mm, flip angle = 55°, voxel size = 2.3mm isotropic, 5x multiband acceleration. We confirmed that no subjects fell asleep with a self-report questionnaire administered after the scanning protocol.

RS-fMRI Preprocessing Procedures

RS-fMRI preprocessing was conducted within FSL, NiPy, and AFNI. Structural scans were registered to the MNI152 template (59) using affine and nonlinear transformations conducted in FSL. Functional image preprocessing included simultaneous 4-D motion and slice-timing correction (60), brain extraction, alignment of

subject's functional images to their anatomical scan using a boundary-based registration algorithm (61), and a one-step nonlinear warp to MNI152 space that concatenated functional-to structural, structural-to-MNI152, and fieldmap unwarping transformations. To mitigate motion-related artifacts we used ICA-AROMA (62), a data-driven classification algorithm that identifies and removes spatiotemporal components likely to reflect head movement. RS-fMRI data were not spatially smoothed for analysis (Supplemental Methods; ,63).

Analytic Approach

Whole-brain Functional Connectivity and ALFF Analyses

We performed whole-brain FC analyses (see Supplemental Methods for details) to identify resting-state network signatures of BPD across levels of the network. We first constructed undirected FC matrices among 421 regions/nodes using a custom-built parcellation covering cortex, striatum, thalamus, and amygdala [43, 64–66; see Fig S2]. Given our interest in network segregation and integration, nodes were assigned to either the default mode (DMN), fronto-parietal (FPN), salience (SN), dorsal attention (DAN), sommato-motor (SomMot), visual (Vis), or cortico-limbic network (Limbic), based on the previously validated modular structure of the cortical and striatal parcellations (64,65,67).

To test for group differences in global FC and ALFF, we compared the strength centrality and global ALFF distributions of the two groups using mixed-effects regression (see Supplemental Methods). We calculated graph measures of global FC (modularity, characteristic path length, transitivity, global efficiency, diameter) and fit separate regression models predicting global graph metrics by group membership, age, and their interaction. We then computed nodal FC measures and ALFF for all brain regions (see Supplemental Methods). In a series of nine logistic ridge regression models, we tested which regional connectivity measures were the most potent predictors of group status; these analyses included graph measures for each region as simultaneous predictors (see Supplemental Methods). Nodal measures included strength centrality, seven separate network-specific strength centrality (NSSC) scores, and ALFF. The NSSC measures corresponded to intra- and inter-network FC with specific networks. For nodal logistic ridge regression analyses we set a

conservative alpha level of .005.

As detailed below, we found strong evidence for widespread hyperconnectivity of the R daIns in BPD. This result motivated a post-hoc analysis on all edges incident to this region, testing for edges with significant group or group-by-age effects. The focal edge analysis provided a more fine-grained test of *which* edges contributed most to group differences in summary statistics such as nodal centrality. Specifically, in a logistic ridge regression, we regressed group status on incident edge values and their interactions with age.

Effective Connectivity Among Target Regions

Initial analyses revealed pivotal group differences in FC/ALFF in R daIns, TPJ, and several (primarily parietal) DAN regions. Subsequent analyses sought to understand how these effects could be understood in terms of EC amongst these regions. We used the recently developed Latent Variable Group Iterative Multiple Model Estimation (LV-GIMME; 44,68,69) algorithm to estimate EC between R TPJ, daIns, and a latent variable capturing shared signal amongst DAN regions (see Supplemental Methods). We additionally allowed for subgroup-specific edges to be estimated based on clinical group status (69). After fitting LV-GIMME to nodal time series, we extracted model coefficients as group-level directed edge values and ran separate linear regressions testing for group and group-by-age effects in the strength of EC.

Path Models Linking EC and ALFF

Building on results from EC estimation, we tested whether the relationship between DAN_{ALFF}[3] and $daIns_{ALFF}$/TPJ_{ALFF} were mediated by EC between these regions[4]. For example, while $daIns_{ALFF}$ and DAN_{ALFF} levels showed an inverse pattern of group-level effects, we directly considered whether parametric increases in daIns daIns→DAN_{EC} inversely scales with DAN_{ALFF} (which would demonstrate an "ALFF suppression" effect).

[3] Given that ALFF effects in DAN were spread across a wide swath of parietal and frontal eye field regions (Fig S6, Table S3), we were more interested in a shared network-level score for ALFF. We fit a single factor EFA to ALFF scores amongst DAN regions with significant group differences and extracted factor scores to be used at the dependent variable in subsequent analyses. Details including bivariate correlations amongst DAN nodes and factor loadings are detailed in Supplemental Materials.

[4] For ease of communication, for the rest of the manuscript we denote effective connectivity between two regions with an arrow and "EC" subscript, and functional connectivity between two regions/networks with a dash and "FC" subscript (e.g. EC from daIns to DAN denoted as daIns→DAN_{EC}, where undirected FC is denoted daIns↔DAN_{FC})

We fit three path models to these variables in Mplus using Bayesian parameter estimation (details in Supplemental Methods; 69–71). In the first two models (Fig. 2a-b), we fit parallel dual-mediation path models in which the relationship between $daIns_{ALFF}$/TPJ_{ALFF} and DAN_{ALFF} was mediated by both daIns/TPJ→DAN_{EC} and daIns/TPJ↔DAN_{FC}, respectively (Fig. 2a-b). The inclusion of FC and EC measures tested the specificity and predictive power of directed and undirected connectivity. In a final model (Fig. 2c), we tested whether TPJ-related variables were predicted by daIns→TPJ_{EC}. This path model specifically adjudicated whether TPJ_{ALFF} and/or TPJ connectivity were better explained as a downstream effect of daIns hyperactivity/connectivity.

Associations with BPD Symptom Domains

Finally, we tested which BPD symptom dimensions were uniquely associated with ALFF impairment in DAN. We fit a series of linear models using each BPQ subscale: $DAN_{ALFF} = \beta_0 + \beta_1 BPQ_{scaleX} + \beta_2 \overline{ALFF}$. However, we were more interested in the unique relevance of specific BPQ subscales given high associations among symptom domains (*r*'s > .7). To test conditional associations of BPQ subscales with DAN ALFF we fit a single multiple regression predicting levels of DAN ALFF by all subscales of the BPQ and average ALFF levels per subject[5].

Results

Whole-brain functional connectivity and ALFF

We found no evidence of significant group or group-by-age differences in global network characteristics (all *p*'s > .05; Table S2, Figs S4-5). Nodal analyses, however, revealed an array of findings across intrinsic networks (Table S3, Fig S6). The primary goal of our nodal analyses was to determine group and group x age differences in FC/ALFF across regions.

We identified three robust patterns in intrinsic network structure that discriminated the BPD group from the control group (Table S3, Fig S6). First, R dorsal aIns (daIns) showed strong, widespread hyperconnectivity

[5] This allowed us to test which specific BPD symptom domains explain significant variability in DAN ALFF, while accounting for their correlation with one another. To allay concerns about multicollinearity and the interpretability of partial betas, we report a dominance analysis in order to test for the incremental predictive ability of BPQ subscales (73). Results confirm that the regressor with the largest partial beta in our joint model induces the greatest average increase the model R^2 across nested sub-models (Table 3).

to six of seven[6] intrinsic networks. Most notably, R daIns↔DAN_{FC} was substantially stronger in the BPD group compared to controls (t = 4.55, p < .0001), controlling for all nodes' $NSSC_{DAN}$ scores. In addition, $daIns_{ALFF}$ was significantly higher in the BPD group (t = 3.76, p < .001). Second, we found a pattern of hypoconnectivity in R TPJ, as indicated by lower strength centrality in the BPD group (t = -2.99, p < .005). Third, we found lower ALFF in the BPD group across parietal nodes in the DAN (all p's < .005).

We conducted a post-hoc ridge regression of all edges connected to daIns[7]. This analysis revealed hyperconnectivity between R daIns and 11 DAN regions (Table S4, all p's < .005), suggesting a broad pattern of hyperconnectivity between daIns and DAN. Parietal DAN regions with lower ALFF overlapped considerably with nodes exhibiting heightened connectivity with daIns (Table S6, Fig S7).

Effective Connectivity Amongst Target Regions

Whole-brain FC/ALFF effects suggested a robust pattern of heightened daIns↔DAN_{FC} coupled with impaired DAN_{ALFF} in the BPD group. However, these analyses cannot reveal the direction of information flow between daIns and DAN. Given insula's status as a major "outflow hub" (18), we interrogated if heightened daIns↔DAN_{FC} could be better understood in terms daIns→DAN_{EC}, rather than DAN→$daIns_{EC}$. To test this hypothesis, we estimated EC among R daIns, TPJ, and 15 selected DAN regions using LV-GIMME (Fig 1). DAN regions were selected based on the unison of regions with lower ALFF *or* heightened FC to daIns (details in Supplemental Materials).

To capture the shared signal among parietal regions in DAN, we fit a latent variable model to their timeseries with LV-GIMME. Results demonstrated that daIns had a directed influence on both DAN and R TPJ (Fig 1). Further, LV-GIMME detected TPJ→DAN_{EC} in HCs that was not present in the BPD group. Linear

[6] The only network that did not appear to show significantly heightened FC to daIns in the BPD group was the Limbic network. We note that this network showed had a remarkably weaker edge strength distribution compared to the other six networks (visually depicted in Figure S3). This network is comprised primarily of inferior temporal and orbitofrontal regions and thus the regional timeseries are likely much noisier do to susceptibility artifacts in fMRI data.

[7] After our mild consensus thresholding procedure (see Supplemental Materials), 26 edges connected to daIns were removed, leaving 394 remaining edges to investigate in our edge analysis.

models indicated that daIns→DAN_{EC} and daIns→TPJ_{EC} were significantly higher in borderline participants (t_{DAN} = 5.27, p_{DAN} < .001; t_{TPJ} = 2.04, p_{TPJ} = .04; Table S7).

Path Models Linking EC and ALFF

Having established group-level increases in daIns→DAN_{EC} and daIns→TPJ_{EC} and widespread lower DAN_{ALFF} in the BPD group, we integrated these findings with a set of multivariate path analyses. In our daIns→DAN path model (Table S8, Fig 2a) we found modest evidence that DAN_{ALFF} was negatively associated with $daIns_{ALFF}$ (p = 0.05) and daIns→DAN_{EC} (p = 0.06), but not daIns↔DAN_{FC} (p = 0.83), controlling for subject-level average FC and ALFF. Further, daIns→DAN_{EC} was positively associated with $daIns_{ALFF}$ (p < 0.001). We found limited support that daIns→DAN_{EC} mediates the relationship between $daIns_{ALFF}$ and DAN_{ALFF} (p = 0.07). In a parallel model (TPJ→DAN, Fig 2b), we tested the associations between TPJ and DAN connectivity and ALFF. We found that TPJ→DAN_{EC} was associated with higher DAN_{ALFF} (p = 0.02). DAN_{ALFF} was not associated with TPJ_{ALFF} (p = 0.38) or TPJ↔DAN_{FC} (p = 0.73). Further, TPJ_{ALFF} was associated with higher TPJ→DAN_{EC} (p < 0.001) and TPJ↔DAN_{FC} (p < 0.001). The association between TPJ_{ALFF} and DAN_{ALFF} was fully mediated by TPJ→DAN_{EC} (p = 0.02).

In our daIns→TPJ→DAN model (Table 2, Fig 2c), we built upon the TPJ→DAN model[8] by demonstrating that TPJ→DAN_{EC} depends on daIns→TPJ_{EC}. While daIns→TPJ_{EC} did not directly predict TPJ→DAN_{EC} (p = 0.74), or TPJ↔DAN_{FC} (p = 0.17), it significantly predicted weaker TPJ_{ALFF} (p = 0.02). In turn, TPJ_{ALFF} fully mediated the relationship between daIns→TPJ_{EC} and both TPJ→DAN_{EC} (p = 0.02) and TPJ↔DAN_{FC} (p = 0.02).

Associations of connectivity measures with BPD Symptom Domains

EC and path analyses demonstrated that lower DAN_{ALFF} in the BPD group is a downstream effect of differential daIns→DAN_{EC} and TPJ→DAN_{EC}. Building on this, we sought to test which borderline symptom domains were most associated with DAN_{ALFF} impairment. In unconditional models, nearly every BPQ subscale

[8] Before moving to interpreting newly introduced daIns paths we confirmed that paths that were present in both models 2 and 3 were nearly identical in terms of parameter values and significance values (Fig 2, Tables S8-9).

was negatively associated with DAN_{ALFF} (Table 3). However, in a single conditional model, the negative association between DAN_{ALFF} and the affective instability subscale remained significant, while the other subscales were not (all *p*'s > .19, Table 3).

Discussion

BPD symptoms often emerge during adolescence (2), a period associated with major neurodevelopmental changes. In a sample of adolescents and young adults with BPD symptoms, we found that right dorsal anterior insula (R daIns) was hyperactive (ALFF) and hyperconnected (FC and EC) to DAN relative to matched controls. We also found hypoactivity across parietal regions in DAN in BPD participants. Path analyses revealed that heightened $daIns_{ALFF}$ (53) bolstered daIns→DAN_{EC}. Importantly, heightened daIns→DAN_{EC} negatively predicted DAN_{ALFF} over and above daIns↔DAN_{FC}. Our findings suggest that blunted resting-state activity in DAN may be a useful biomarker of BPD that reflects differential inputs from SN regions. Comparing across BPD symptom domains, diminished DAN_{ALFF} was most strongly associated with affective instability. Although we allowed age to moderate these effects, our primary results were consistent across the age range of the sample (13–30). Thus, differences in daIns connectivity and DAN_{ALFF} may be a characteristic of BPD more generally.

We found that lower DAN_{ALFF} was differentially predicted by EC from two key SN nodes: whereas daIns→DAN_{EC} suppressed DAN_{ALFF}, TPJ→DAN_{EC} enhanced DAN_{ALFF}. Although DAN_{ALFF} was bolstered by TPJ→DAN_{EC}, TPJ_{ALFF} was itself suppressed by daIns→TPJ_{EC} in the BPD group. Thus, while daIns→DAN_{EC} and TPJ→DAN_{EC} play competing roles in modulating DAN_{ALFF}, our analyses suggest the primacy of daIns in modulating activity in both DAN and TPJ. These results provide compelling evidence for aberrant integration of SN and DAN in BPD. A more nuanced interpretation is that abnormal intra-network communication within the SN (stemming from increased daIns→TPJ_{EC}) leads to an imbalance in the strength of inputs from anterior (insula) vs posterior (TPJ) nodes of the SN to DAN.

aIns is a core node of SN that supports cognitive-emotional processing via attentional shifts that accord with task-related goals by assigning salience to behaviorally relevant cues (15,17). Its rapid integration of

visceral/homeostatic, emotional, social, cognitive, and sensory signals place aIns in a unique position to control the ongoing assignment of resources to networks responsible for the processing of exogenous cues or internal self-referential information (15,18,20). In previous studies daIns showed the strongest pattern of co-activation with higher-order cognitive networks (FPN, DAN) and was more strongly associated with switching tasks, whereas ventral anterior and posterior insula co-activate with affective and sensorimotor processing networks, respectively (21). This evidence aligns well with our finding of greater daIns↔DAN_{FC} in the BPD group, suggesting that hyperactivity in this region has the greatest ability to influence cognitive/executive functions.

We also found that R TPJ, a node of the posterior SN, showed widespread, though less pronounced, hypoconnectivity across networks. Prior fMRI studies of BPD have found that R TPJ is hypoactivated across tasks measuring self/other differentiation, perspective-taking, and social feedback processing (29,74–76). These findings align well with R TPJ's hypothesized role in theory of mind and mentalization (77) and more recent claims that TPJ is crucial in constructing social contexts (78) and representing social agents and their intentions (79). Hypoconnectivity of R TPJ in our data may reflect difficulties in perspective-taking and mentalizing associated with adolescent (80–82) and adult (83) BPD. However, TPJ is also linked to the more universal task of contextual updating and adjusting top-down expectations (84), providing an intriguing clue for a domain-general functional impairment in BPD that would have direct implications for social-cognitive functioning. The hyper-vs hypo-connectivity dissociation within SN (daIns versus TPJ) helps to reconcile previous conflicting findings of SN connectivity in BPD. One ICA study found increased FC of canonical/anterior SN, including insula and dACC (34), where another study found hypoconnectivity in a more widespread "social salience network" that included canonical SN nodes *and* TPJ (33). While R daIns and TPJ appear to form a functional circuit (i.e. SN), intra-SN daIns→TPJ_{EC} impairs TPJ_{ALFF}, leading to downstream impairment of inter-network TPJ→DAN_{EC} in BPD participants.

DAN is involved in the control of goal-oriented/top-down selective attention (85,86) and plays a central role in prioritizing sensory inputs for further processing, including saccades towards high priority stimuli (87). Extending this notion, parietal DAN nodes construct a "priority map" of visual input by integrating top-down

signals relevant to goals and expectations with a compressed representation of sensory features. In turn, priority maps bias neural activity in primary sensory networks and govern information-seeking behaviors, particularly saccades (88–90). Lower DAN_{ALFF} in BPD points to a diminished capacity to integrate higher-order goal representations to guide attention. Thus, attentional orientation towards stimuli that are associated with abstract goals may be overpowered by daIns-generated switch signals to brief stimuli with high associative salience. This account is partially consistent with the triple network model, which posits that altered salience processing in aIns underlies key dysfunctional interactions between FPN, SN, and DMN. However, we found stronger evidence of aberrant SN↔DAN_{FC}, providing an intriguing extension of the triple network model in borderline personality (23). Our data supports a slightly different view that aberrant SN functioning has greater direct implications on selective or transient attentional control implemented by DAN (91), which shows anatomical and functional dissociations from FPN (39,92).

We propose that heightened daIns→DAN_{EC} in BPD may reflect a vulnerability to "hijacking" of goal-directed, transient attention by the aIns. Heightened activity and connectivity of daIns may increase attentional switches among competing priorities or immediate needs in young people with BPD symptoms. This attentional hijacking hypothesis, if corroborated and extended in subsequent research, could provide a circuit-based account of attentional biases in BPD, characterized by faster saccades to and longer fixations on the eyes of emotional faces (93–95). While previous FC studies of SN-DAN interactions remain equivocal on the directionality of influence between these networks, our LV-GIMME analysis specifically tested the hypothesis that SN nodes primarily act on DAN. Our analysis suggests that in individuals with BPD symptoms, TPJ_{ALFF} and DAN_{ALFF} both fall prey to hijacking by daIns. A high-level conclusion from our analyses is that heightened switch-signaling from daIns impairs DAN_{ALFF} both directly (daIns→DAN_{EC}) and indirectly vis-à-vis blunted TPJ→DAN_{EC}. Moreover, weaker DAN_{ALFF} was particularly associated with heightened affective instability in our study, suggesting that disrupted intrinsic activity in DAN enhances vulnerability to negative emotion (96).

To our knowledge this is the first whole-brain rsFC study in a sample of adolescents and young adults with BPD symptoms, allowing for an initial description of intrinsic connectivity during a period of heightened

vulnerability. Second, our study combined well-validated parcellations of the cortex, striatum, amygdala, and thalamus, allowing for a fine-grained analysis of whole-brain FC. Third, our network neuroscience approach leveraged NSSC scores, allowing for focal tests of intra- and inter-network connectivity that overcome the limitations of broader between-network connectivity measures such as participation coefficient (97). Fourth, we analyzed ALFF to uncover differential contributions of intrinsic connectivity and intrinsic activity to the functional network profile of BPD. Fifth, our LV-GIMME analysis reflects a state-of-the-art approach to measuring the directionality of connectivity when there are shared signals (here, nodes within DAN) in a network (98).

While our results suggest a novel "attentional hijacking" hypothesis of BPD, in the absence of goal-directed attentional control tasks, this hypothesis remains speculative. Future studies can directly test this hypothesis in task-based studies that manipulate exogenous and/or internal shifts of attention. Our primary findings emphasize group differences that were consistent across individuals between ages 13 and 30, and longitudinal assessments with clinical comparison groups are necessary to directly investigate within-person connectivity *changes* over adolescence. Likewise, replicating these findings in a sample of older adults with BPD symptoms would clarify whether daIns connectivity plays a major role in DAN intrinsic activity across the lifespan.

In summary, we found that intrinsic hypoactivity of DAN plays a pivotal role in the expression of borderline personality symptoms, particularly affective instability, in young people. We suggest that this pattern may represent an insula-driven attentional hijacking process whereby daIns interferes with goal-directed attentional control in DAN both directly and indirectly via impaired TPJ connectivity. This account builds on evidence that the aIns implements attentional switches in response to dynamically changing homeostatic needs on short timescales (13). If hyperconnectivity of the daIns with DAN regions supports rapid attentional shifts, our findings may help explain the well-documented sensitivity to brief emotional cues that form a core feature of borderline personality (99,100). We hope that future studies extend these findings to refine a circuit-based

account of borderline symptoms in adolescents that can inform early intervention treatments in this high-risk, yet understudied, population.

References

1. Sharp C, Vanwoerden S, Wall K (2018): Adolescence as a Sensitive Period for the Development of Personality Disorder. *Psychiatric Clinics* 41: 669–683.

2. Zanarini MC, Frankenburg FR, Ridolfi ME, Jager-Hyman S, al et (2006): Reported Childhood Onset of Self-Mutilation Among Borderline Patients. *Journal of Personality Disorders* 20: 9–15.

3. Shulman EP, Smith AR, Silva K, Icenogle G, Duell N, Chein J, Steinberg L (2016): The dual systems model: Review, reappraisal, and reaffirmation. *Developmental Cognitive Neuroscience* 17: 103–117.

4. Lei X, Zhong M, Liu Y, Jin X, Zhou Q, Xi C, *et al.* (2017): A resting-state fMRI study in borderline personality disorder combining amplitude of low frequency fluctuation, regional homogeneity and seed based functional connectivity. *Journal of Affective Disorders* 218: 299–305.

5. Lei X, Liao Y, Zhong M, Peng W, Liu Q, Yao S, *et al.* (2018): Functional Connectivity Density, Local Brain Spontaneous Activity, and Their Coupling Strengths in Patients With Borderline Personality Disorder. *Front Psychiatry* 9. https://doi.org/10.3389/fpsyt.2018.00342

6. Salvador R, Vega D, Pascual JC, Marco J, Canales-Rodríguez EJ, Aguilar S, *et al.* (2016): Converging Medial Frontal Resting State and Diffusion-Based Abnormalities in Borderline Personality Disorder. *Biological Psychiatry* 79: 107–116.

7. Fair DA, Dosenbach NUF, Church JA, Cohen AL, Brahmbhatt S, Miezin FM, *et al.* (2007): Development of distinct control networks through segregation and integration. *PNAS* 104: 13507–13512.

8. Marek S, Hwang K, Foran W, Hallquist MN, Luna B (2015): The Contribution of Network Organization and Integration to the Development of Cognitive Control. *PLOS Biology* 13: e1002328.

9. Hwang K, Hallquist MN, Luna B (2013): The Development of Hub Architecture in the Human Functional Brain Network. *Cereb Cortex* 23: 2380–2393.

10. Engelhardt LE, Harden KP, Tucker-Drob EM, Church JA (2019): The neural architecture of executive functions is established by middle childhood. *NeuroImage* 185: 479–489.

11. He W, Sowman PF, Brock J, Etchell AC, Stam CJ, Hillebrand A (2019): Increased segregation of functional networks in developing brains. *NeuroImage* 200: 607–620.

12. Seeley WW, Menon V, Schatzberg AF, Keller J, Glover GH, Kenna H, *et al.* (2007): Dissociable Intrinsic Connectivity Networks for Salience Processing and Executive Control. *J Neurosci* 27: 2349–2356.

13. Seeley WW (2019): The Salience Network: A Neural System for Perceiving and Responding to Homeostatic Demands. *J Neurosci* 39: 9878–9882.

14. Kolskår KK, Alnæs D, Kaufmann T, Richard G, Sanders A-M, Ulrichsen KM, *et al.* (2018): Key Brain Network Nodes Show Differential Cognitive Relevance and Developmental Trajectories during Childhood and Adolescence. *eNeuro*. https://doi.org/10.1523/ENEURO.0092-18.2018

15. Menon V, Uddin LQ (2010): Saliency, switching, attention and control: a network model of insula function. *Brain Struct Funct* 214: 655–667.

16. Uddin LQ, Yeo BTT, Spreng RN (2019): Towards a Universal Taxonomy of Macro-scale Functional Human Brain Networks. *Brain Topogr* 32: 926–942.

17. Uddin LQ (2015): Salience processing and insular cortical function and dysfunction. *Nature Reviews Neuroscience* 16: 55–61.

18. Sridharan D, Levitin DJ, Menon V (2008): A critical role for the right fronto-insular cortex in switching between central-executive and default-mode networks. *PNAS* 105: 12569–12574.

19. Li R, Zhang S, Yin S, Ren W, He R, Li J (2018): The fronto-insular cortex causally mediates the default-mode and central-executive networks to contribute to individual cognitive performance in healthy elderly. *Human Brain Mapping* 39: 4302–4311.

20. Craig AD (2009): How do you feel — now? The anterior insula and human awareness. *Nat Rev Neurosci* 10: 59–70.

21. Chang LJ, Yarkoni T, Khaw MW, Sanfey AG (2013): Decoding the Role of the Insula in Human Cognition: Functional Parcellation and Large-Scale Reverse Inference. *Cereb Cortex* 23: 739–749.

22. Uddin LQ, Nomi JS, Hébert-Seropian B, Ghaziri J, Boucher O (2017): Structure and Function of the Human Insula. *Journal of Clinical Neurophysiology* 34: 300.

23. Menon V (2011): Large-scale brain networks and psychopathology: a unifying triple network model. *Trends in Cognitive Sciences* 15: 483–506.

24. Bassett DS, Xia CH, Satterthwaite TD (2018): Understanding the Emergence of Neuropsychiatric Disorders With Network Neuroscience. *Biological Psychiatry: Cognitive Neuroscience and Neuroimaging* 3: 742–753.

25. Peters SK, Dunlop K, Downar J (2016): Cortico-Striatal-Thalamic Loop Circuits of the Salience Network: A Central Pathway in Psychiatric Disease and Treatment. *Front Syst Neurosci* 10. https://doi.org/10.3389/fnsys.2016.00104

26. Palaniyappan L, Liddle PF (2012): Does the salience network play a cardinal role in psychosis? An emerging hypothesis of insular dysfunction. *Journal of Psychiatry & Neuroscience* 37: 17–27.

27. Uddin LQ (2021): Brain Mechanisms Supporting Flexible Cognition and Behavior in Adolescents With Autism Spectrum Disorder. *Biological Psychiatry* 89: 172–183.

28. Minzenberg MJ, Fan J, New AS, Tang CY, Siever LJ (2007): Fronto-limbic dysfunction in response to facial emotion in borderline personality disorder: An event-related fMRI study. *Psychiatry Research: Neuroimaging* 155: 231–243.

29. Beeney JE, Hallquist MN, Ellison WD, Levy KN (2016): Self–other disturbance in borderline personality disorder: Neural, self-report, and performance-based evidence. *Personality Disorders: Theory, Research, and Treatment* 7: 28–39.

30. Silbersweig D, Clarkin JF, Goldstein M, Kernberg OF, Tuescher O, Levy KN, *et al.* (2007): Failure of Frontolimbic Inhibitory Function in the Context of Negative Emotion in Borderline Personality Disorder. *AJP* 164: 1832–1841.

31. Ruocco AC, Amirthavasagam S, Choi-Kain LW, McMain SF (2013): Neural Correlates of Negative Emotionality in Borderline Personality Disorder: An Activation-Likelihood-Estimation Meta-Analysis. *Biological Psychiatry* 73: 153–160.

32. Soloff PH, White R, Omari A, Ramaseshan K, Diwadkar VA (2015): Affective context interferes with brain responses during cognitive processing in borderline personality disorder: fMRI evidence. *Psychiatry Research: Neuroimaging* 233: 23–35.

33. Das P, Calhoun V, Malhi GS (2014): Bipolar and borderline patients display differential patterns of functional connectivity among resting state networks. *NeuroImage* 98: 73–81.

34. Doll A, Sorg C, Manoliu A, Meng C, Wöller A, Förstl H, *et al.* (2013): Shifted intrinsic connectivity of central executive and salience network in borderline personality disorder. *Front Hum Neurosci* 7. https://doi.org/10.3389/fnhum.2013.00727

35. Sarkheil P, Ibrahim CN, Schneider F, Mathiak K, Klasen M (2019): Aberrant functional connectivity profiles of brain regions associated with salience and reward processing in female patients with borderline personality disorder. *Brain Imaging and Behavior*. https://doi.org/10.1007/s11682-019-00065-z

36. Paulus MP, Stein MB (2006): An Insular View of Anxiety. *Biological Psychiatry* 60: 383–387.

37. Uddin LQ, Menon V (2009): The anterior insula in autism: Under-connected and under-examined. *Neuroscience & Biobehavioral Reviews* 33: 1198–1203.

38. Goodkind M, Eickhoff SB, Oathes DJ, Jiang Y, Chang A, Jones-Hagata LB, *et al.* (2015): Identification of a common neurobiological substrate for mental illness. *JAMA Psychiatry* 72: 305–315.

39. Witt ST, van Ettinger-Veenstra H, Salo T, Riedel MC, Laird AR (2021): What Executive Function Network is that? An Image-Based Meta-Analysis of Network Labels. *Brain Topogr* 34: 598–607.

40. Vossel S, Geng JJ, Fink GR (2014): Dorsal and Ventral Attention Systems: Distinct Neural Circuits but Collaborative Roles. *Neuroscientist* 20: 150–159.

41. Bassett DS, Sporns O (2017): Network neuroscience. *Nat Neurosci* 20: 353–364.

42. Rubinov M, Sporns O (2010): Complex network measures of brain connectivity: Uses and interpretations. *NeuroImage* 52: 1059–1069.

43. Hallquist MN, Hillary FG (2018): Graph theory approaches to functional network organization in brain disorders: A critique for a brave new small-world. *Network Neuroscience* 1–26.

44. Gates KM, Molenaar PCM (2012): Group search algorithm recovers effective connectivity maps for individuals in homogeneous and heterogeneous samples. *NeuroImage* 63: 310–319.

45. Friston KJ (2011): Functional and Effective Connectivity: A Review. *Brain Connectivity* 1: 13–36.

46. Friston K, Moran R, Seth AK (2013): Analysing connectivity with Granger causality and dynamic causal modelling. *Current Opinion in Neurobiology* 23: 172–178.

47. Hall NT, Hallquist MN (2022): Dissociation of basolateral and central amygdala effective connectivity predicts the stability of emotion-related impulsivity in adolescents and emerging adults with borderline personality symptoms: a resting-state fMRI study. *Psychological Medicine* 1–15.

48. New AS, Hazlett EA, Buchsbaum MS, Goodman M, Mitelman SA, Newmark R, *et al.* (2007): Amygdala–Prefrontal Disconnection in Borderline Personality Disorder. *Neuropsychopharmacology* 32: 1629–1640.

49. Schulze L, Schmahl C, Niedtfeld I (2016): Neural Correlates of Disturbed Emotion Processing in Borderline Personality Disorder: A Multimodal Meta-Analysis. *Biol Psychiatry* 79: 97–106.

50. Soloff PH, Meltzer CC, Becker C, Greer PJ, Kelly TM, Constantine D (2003): Impulsivity and prefrontal hypometabolism in borderline personality disorder. *Psychiatry Research: Neuroimaging* 123: 153–163.

51. Biswal BB, Yetkin FZ, Haughton VM, Hyde JS (1995): Functional connectivity in the motor cortex of resting human brain using echo-planar MRI. *Magnetic Resonance in Medicine* 34: 537–541.

52. Zang YF, He Y, Zhu CZ, Cao QJ, Sui MQ, Liang M, *et al.* (2007): Altered baseline brain activity in children with ADHD revealed by resting-state functional MRI. *Brain Dev* 29: 83–91.

53. Tomasi D, Wang G-J, Volkow ND (2013): Energetic cost of brain functional connectivity. *PNAS* 110: 13642–13647.

54. Kurcyus K, Annac E, Hanning NM, Harris AD, Oeltzschner G, Edden R, Riedl V (2018): Opposite Dynamics of GABA and Glutamate Levels in the Occipital Cortex during Visual Processing. *J Neurosci* 38: 9967–9976.

55. Pfohl B, Blum N, Zimmerman M (1997): *Structured Interview for DSM-IV Personality: SIDP-IV*. American Psychiatric Pub.

56. First MB, Spitzer RL, Gibbon M, Williams JB (1997): *User's Guide for the Structured Clinical Interview for DSM-IV Axis I Disorders SCID-I: Clinician Version*. American Psychiatric Pub.

57. Clifton A, Pilkonis PA (2007): Evidence for a single latent class of Diagnostic and Statistical Manual of Mental Disorders borderline personality pathology. *Comprehensive Psychiatry* 48: 70–78.

58. Poreh AM, Rawlings D, Claridge G, Freeman JL, Faulkner C, Shelton C (2006): The BPQ: A Scale for the Assessment of Borderline Personality Based on DSM-IV Criteria. *Journal of Personality Disorders* 20: 247–260.

59. Fonov VS, Evans AC, McKinstry RC, Almli CR, Collins DL (2009): Unbiased nonlinear average age-appropriate brain templates from birth to adulthood. *NeuroImage* Supplement 1: S102.

60. Roche A (2011): A Four-Dimensional Registration Algorithm With Application to Joint Correction of Motion and Slice Timing in fMRI. *IEEE Transactions on Medical Imaging* 30: 1546–1554.

61. Greve DN, Fischl B (2009): Accurate and robust brain image alignment using boundary-based registration., Accurate and Robust Brain Image Alignment using Boundary-based Registration. *Neuroimage* 48, 48: 63, 63–72.

62. Pruim RHR, Mennes M, van Rooij D, Llera A, Buitelaar JK, Beckmann CF (2015): ICA-AROMA: A robust ICA-based strategy for removing motion artifacts from fMRI data. *NeuroImage* 112: 267–277.

63. Alakörkkö T, Saarimäki H, Glerean E, Saramäki J, Korhonen O (2017): Effects of spatial smoothing on functional brain networks. *Eur J Neurosci* 46: 2471–2480.

64. Schaefer A, Kong R, Gordon EM, Laumann TO, Zuo X-N, Holmes AJ, *et al.* (2018): Local-Global Parcellation of the Human Cerebral Cortex from Intrinsic Functional Connectivity MRI. *Cereb Cortex* 28: 3095–3114.

65. Choi EY, Yeo BTT, Buckner RL (2012): The organization of the human striatum estimated by intrinsic functional connectivity. *J Neurophysiol* 108: 2242–2263.

66. Behrens TEJ, Johansen-Berg H, Woolrich MW, Smith SM, Wheeler-Kingshott C a. M, Boulby PA, *et al.* (2003): Non-invasive mapping of connections between human thalamus and cortex using diffusion imaging. *Nat Neurosci* 6: 750–757.

67. Yeo BTT, Krienen FM, Sepulcre J, Sabuncu MR, Lashkari D, Hollinshead M, *et al.* (2011): The organization of the human cerebral cortex estimated by intrinsic functional connectivity. *Journal of Neurophysiology* 106: 1125–1165.

68. Gates KM, Fisher ZF, Bollen KA (2020): Latent variable GIMME using model implied instrumental variables (MIIVs). *Psychological Methods* 25: 227–242.

69. Henry TR, Feczko E, Cordova M, Earl E, Williams S, Nigg JT, *et al.* (2019): Comparing directed functional connectivity between groups with confirmatory subgrouping GIMME. *NeuroImage* 188: 642–653.

70. Asparouhov T, Muthen B (2010): Bayesian Analysis Using Mplus: Technical Implementation. 38.

71. Hallquist MN, Wiley JF (2018): MplusAutomation: An R Package for Facilitating Large-Scale Latent Variable Analyses in Mplus. *Structural Equation Modeling: A Multidisciplinary Journal* 25: 621–638.

72. Muthén LK, Muthén C (2007): *Mplus: Statistical Analysis with Latent Variables (Version 4.21) [Computer Software*.

73. Budescu DV (1993): Dominance analysis: A new approach to the problem of relative importance of predictors in multiple regression. *Psychological Bulletin* 114: 542–551.

74. Schie CC van, Chiu C-D, Rombouts SARB, Heiser WJ, Elzinga BM (undefined/ed): Stuck in a negative me: fMRI study on the role of disturbed self-views in social feedback processing in borderline personality disorder. *Psychological Medicine* 1–11.

75. Haas BW, Miller JD (2015): Borderline personality traits and brain activity during emotional perspective taking. *Personality Disorders: Theory, Research, and Treatment* 6: 315–320.

76. O'Neill A, D'Souza A, Samson AC, Carballedo A, Kerskens C, Frodl T (2015): Dysregulation between emotion and theory of mind networks in borderline personality disorder. *Psychiatry Research: Neuroimaging* 231: 25–32.

77. Saxe R, Kanwisher N (2003): People thinking about thinking people: The role of the temporo-parietal junction in "theory of mind." *NeuroImage* 19: 1835–1842.

78. Carter RM, Huettel SA (2013): A Nexus Model of the Temporal-Parietal Junction. *Trends Cogn Sci* 17: 328–336.

79. Hill CA, Suzuki S, Polania R, Moisa M, O'Doherty JP, Ruff CC (2017): A causal account of the brain network computations underlying strategic social behavior [no. 8]. *Nature Neuroscience* 20: 1142–1149.

80. Fonagy P, Luyten P, Moulton-Perkins A, Lee Y-W, Warren F, Howard S, *et al*. (2016): Development and Validation of a Self-Report Measure of Mentalizing: The Reflective Functioning Questionnaire. *PLOS ONE* 11: e0158678.

81. Sharp C, Ha C, Carbone C, Kim S, Perry K, Williams L, Fonagy P (2013): Hypermentalizing in adolescent inpatients: treatment effects and association with borderline traits. *J Pers Disord* 27: 3–18.

82. Kalpakci A, Vanwoerden S, Elhai JD, Sharp C (2015): The Independent Contributions of Emotion Dysregulation and Hypermentalization to the "Double Dissociation" of Affective and Cognitive Empathy in Female Adolescent Inpatients With BPD. *Journal of Personality Disorders* 30: 242–260.

83. Euler S, Nolte T, Constantinou M, Griem J, Montague PR, Fonagy P (2019): Interpersonal Problems in Borderline Personality Disorder: Associations with Mentalizing, Emotion Regulation, and Impulsiveness. *Journal of Personality Disorders* 1–17.

84. Geng JJ, Vossel S (2013): Re-evaluating the role of TPJ in attentional control: Contextual updating? *Neuroscience & Biobehavioral Reviews* 37: 2608–2620.

85. Hopfinger JB, Buonocore MH, Mangun GR (2000): The neural mechanisms of top-down attentional control [no. 3]. *Nature Neuroscience* 3: 284–291.

86. Bowling JT, Friston KJ, Hopfinger JB (2020): Top-down versus bottom-up attention differentially modulate frontal–parietal connectivity. *Human Brain Mapping* 41: 928–942.

87. Driver J (2001): A selective review of selective attention research from the past century. *British Journal of Psychology* 92: 53–78.

88. Ptak R (2012): The Frontoparietal Attention Network of the Human Brain: Action, Saliency, and a Priority Map of the Environment. *Neuroscientist* 18: 502–515.

89. Bisley JW, Mirpour K (2019): The neural instantiation of a priority map. *Current Opinion in Psychology* 29: 108–112.

90. Gottlieb J (2012): Attention, Learning, and the Value of Information. *Neuron* 76: 281–295.

91. Corbetta M, Shulman GL (2002): Control of goal-directed and stimulus-driven attention in the brain. *Nat Rev Neurosci* 3: 201–215.

92. Vincent JL, Kahn I, Snyder AZ, Raichle ME, Buckner RL (2008): Evidence for a Frontoparietal Control System Revealed by Intrinsic Functional Connectivity. *Journal of Neurophysiology* 100: 3328–3342.

93. Bertsch K, Krauch M, Stopfer K, Haeussler K, Herpertz SC, Gamer M (2017): Interpersonal Threat Sensitivity in Borderline Personality Disorder: An Eye-Tracking Study. *Journal of Personality Disorders* 31: 647–670.

94. Seitz KI, Leitenstorfer J, Krauch M, Hillmann K, Boll S, Ueltzhoeffer K, *et al.* (2021): An eye-tracking study of interpersonal threat sensitivity and adverse childhood experiences in borderline personality disorder. *Borderline Personality Disorder and Emotion Dysregulation* 8: 2.

95. Kaiser D, Jacob GA, van Zutphen L, Siep N, Sprenger A, Tuschen-Caffier B, *et al.* (2019): Biased Attention to Facial Expressions of Ambiguous Emotions in Borderline Personality Disorder: An Eye-Tracking Study. *Journal of Personality Disorders* 33: 671-S8.

96. Gross JJ (2015): Emotion Regulation: Current Status and Future Prospects. *Psychological Inquiry* 26: 1–26.

97. Guimerà R, Amaral LAN (2005): Cartography of complex networks: modules and universal roles. *J Stat Mech* 2005: P02001.

98. Bolt T, Prince EB, Nomi JS, Messinger D, Llabre MM, Uddin LQ (2018): Combining region- and network-level brain-behavior relationships in a structural equation model. *NeuroImage* 165: 158–169.

99. van Zutphen L, Siep N, Jacob GA, Goebel R, Arntz A (2015): Emotional sensitivity, emotion regulation and impulsivity in borderline personality disorder: A critical review of fMRI studies. *Neuroscience & Biobehavioral Reviews* 51: 64–76.

100. Crowell SE, Beauchaine TP, Linehan MM (2009): A biosocial developmental model of borderline personality: Elaborating and extending Linehan's theory. *Psychol Bull* 135: 495–510.

Figures and Tables

Figure 1

Effective connectivity results

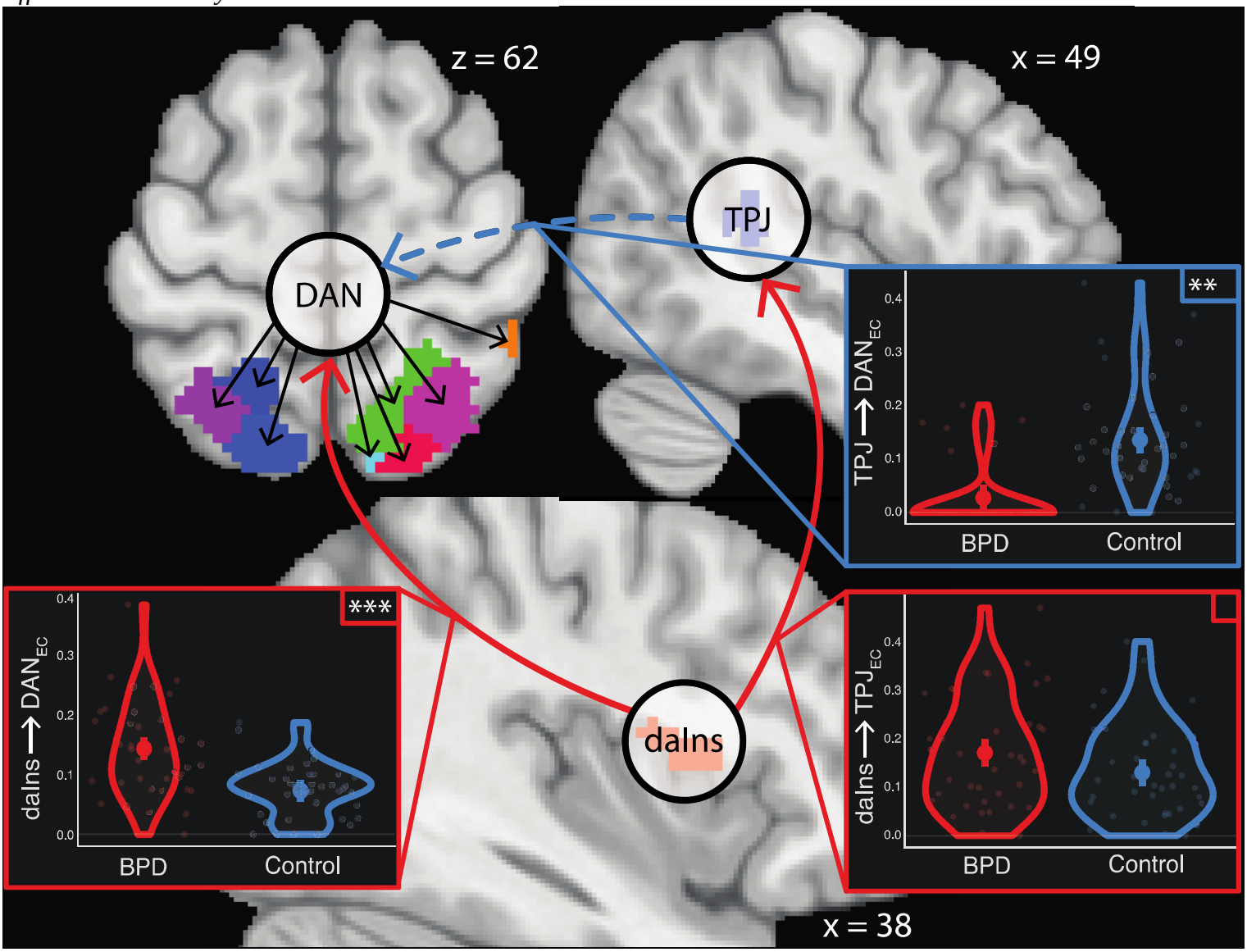

Note. Circles denote BOLD signals fit within LV-GIMME framework. Note that SN nodes (daIns, TPJ) are fit to the nodal timeseries whereas DAN was fit as a network-level latent variable given the strong pattern of shared signal across DAN regions (see Table S6). Red solid arrows denote group-level edges that were significantly higher in the BPD group, where the dashed blue arrow denotes a HC-specific edge from TPJ to DAN. Violin/density plots are overlain on extracted model betas for each edge (e.g. model-predicted edge values) and bolded points denote the expected marginal mean of each edge for each group, averaged over mean FC value (***p < .001, *p < .05; details in Table S7).

Figure 2

Graphical depiction of path models linking daIns, TPJ, and DAN signals

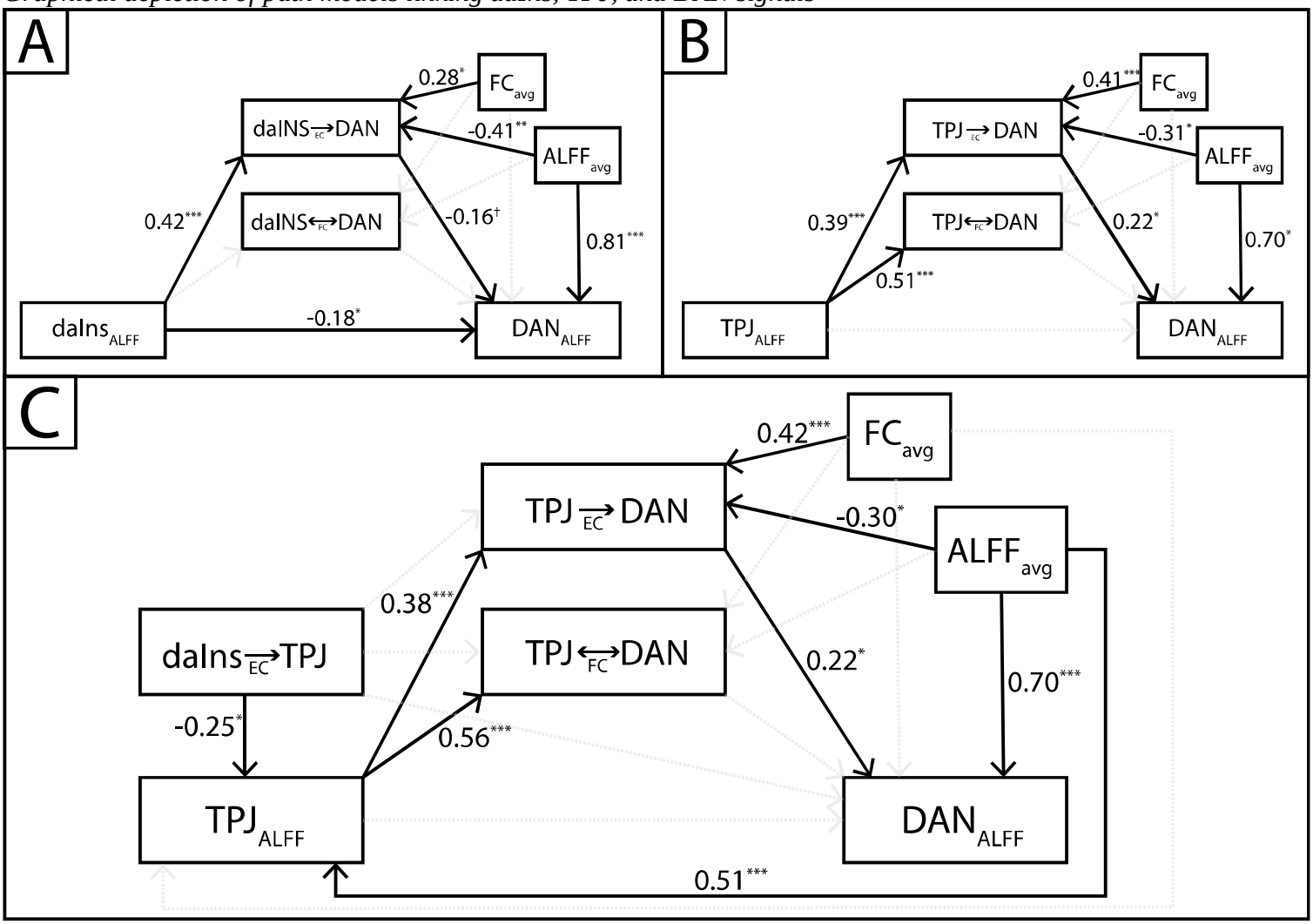

Note. Visual depiction of path models, fit with Bayesian parameter estimation in Mplus. Path values denote standardized estimates. In top left and right panels, we depict parallel dual-mediator path models that tested the ability of SN regions (daIns on left and TPJ on right) FC *and* EC to DAN to mediate the relationship between $daIns_{ALFF}$/TPJ_{ALFF} and DAN_{ALFF}, with both models finding support that EC from both SN regions mediate this relationship and outcompete FC measures in explaining variance in DAN_{ALFF}. In the bottom panel, our combined model builds on the TPJ → DAN model, by showing that EC from daIns to TPJ suppresses TPJ_{ALFF} leading to downstream consequences on TPJ to DAN EC. Details on all three models are reported in Table 3 (combined) and Tables S8-9 (initial parallel mediation models).

Table 1

Sample Characteristics

Characteristic	BPD (*n* = 40)	HC (*n* = 42)
Age (SD)	20.84 (4.42)	20.61 (4.16)
PAI-BOR (SD)	47.3 (9.60)	10.3 (3.99)
Ethnicity		
Hispanic or Latino	3	2
Not Hispanic or Latino	36	40
Not Provided/Missing	1	0
Race		
Caucasian	31	30
African American	3	7
Asian American	2	1
Bi/Multiracial	2	4
Not Provided/Missing	2	0
Average Annual Income		
< $5,000-$19,999	10	11
$20,000-$34,9999	9	7
$35,000 - $59,999	8	5
$60,000 - $99,999	5	6
$100,000 +	3	10
Not Provided/Missing	5	3
Sexuality		
Heterosexual	28	40
Gay/Lesbian	1	1
Bisexual	8	0
Other	1	1
Not Provided/Missing	2	0
Psychiatric Medication		
Any Psychiatric Medication	18	0
SSRI	15	0
SNRI	2	0
Buproprion	3	0
Sedative	5	0
Antipsychotic	0	0
Anticonvulsant	2	0

Note. Samples were sex- and age-matched. PAI-BOR: Personality Assessment Inventory – Borderline subscale.

Table 2

Parameter Table: daIns→TPJ→DAN (Combined) Model

Parameter Type	Outcome	Predictor	Est.s	Lower CI (2.5%)	Upper CI (97.5%)	*p* (two-tailed)
Regression	DAN_{ALFF}	TPJ_{ALFF}	0.034	-0.047	0.116	0.414
		$TPJ \rightarrow DAN_{EC}$	**0.890**	**0.128**	**1.667**	**0.020***
		$TPJ \leftrightarrow DAN_{FC}$	0.014	-0.067	0.094	0.730
		$daIns \rightarrow TPJ_{EC}$	-0.007	-0.661	0.637	0.982
		$\overline{FC}$	-0.308	-2.169	1.563	0.748
		$\overline{ALFF}$	**0.312**	**0.229**	**0.395**	**<0.001****
	$TPJ \rightarrow DAN_{EC}$	**TPJ_{ALFF}**	**0.041**	**0.016**	**0.067**	**0.002****
		$daIns \rightarrow TPJ_{EC}$	-0.039	-0.270	0.190	0.744
		$\overline{FC}$	**1.014**	**0.395**	**1.622**	**0.002****
		$\overline{ALFF}$	**-0.032**	**-0.061**	**-0.004**	**0.026***
	$TPJ \leftrightarrow DAN_{FC}$	**TPJ_{ALFF}**	**0.601**	**0.356**	**0.846**	**<0.001****
		$daIns \rightarrow TPJ_{EC}$	1.547	-0.677	3.755	0.174
		$\overline{FC}$	2.600	-3.339	8.602	0.392
		$\overline{ALFF}$	-0.212	-0.492	0.006	0.132
	TPJ_{ALFF}	**$daIns \rightarrow TPJ_{EC}$**	**-2.370**	**-4.320**	**-0.374**	**0.022***
		$\overline{FC}$	2.350	-3.155	7.819	0.396
		$\overline{ALFF}$	**0.513**	**0.288**	**0.742**	**<0.001****
Connectivity Correlation	**$TPJ \rightarrow DAN_{EC}$**	**$TPJ \leftrightarrow DAN_{FC}$**	**0.044**	**0.026**	**0.070**	**<0.001****
Residual Variances	DAN_{ALFF}		**0.067**	**0.049**	**0.095**	**<0.001****
	$TPJ \rightarrow DAN_{EC}$		**0.009**	**0.006**	**0.012**	**<0.001****
	$TPJ \leftrightarrow DAN_{FC}$		**0.793**	**0.582**	**1.118**	**<0.001****
	TPJ_{ALFF}		**0.675**	**0.499**	**0.945**	**<0.001****
Intercepts	DAN_{ALFF}		**0.494**	**0.042**	**0.954**	**0.032***
	$TPJ \rightarrow DAN_{EC}$		**-0.255**	**-0.399**	**-0.111**	**0.002****
	$TPJ \leftrightarrow DAN_{FC}$		**-2.524**	**-3.956**	**-1.137**	**<0.001****
	TPJ_{ALFF}		**2.707**	**1.570**	**3.848**	**<0.001****
Mediation: Indirect Effects	**$TPJ_{ALFF} \rightarrow TPJ \rightarrow DAN_{EC} \rightarrow DAN_{ALFF}$**		**0.034**	**0.004**	**0.085**	**0.022***
	$TPJ_{ALFF} \rightarrow TPJ \leftrightarrow DAN_{FC} \rightarrow DAN_{ALFF}$		0.008	-0.042	0.059	0.730
	$daIns \rightarrow TPJ_{EC} \rightarrow TPJ_{ALFF} \rightarrow TPJ \rightarrow DAN_{EC}$		**-0.092**	**-0.218**	**-0.010**	**0.024***
	$daIns \rightarrow TPJ_{EC} \rightarrow TPJ_{ALFF} \rightarrow TPJ \leftrightarrow DAN_{FC}$		**-1.374**	**-2.913**	**-0.211**	**0.022***

Table 2

Parameter Table: daIns→TPJ→DAN (Combined) Model

Parameter Type	Outcome	Predictor	Est.s	Lower CI (2.5%)	Upper CI (97.5%)	*p* (two-tailed)

Note. CFI = 0.991, TLI = 0.885, RMSEA = 0.144, Posterior Predictive P-Value = 0.443. Est denotes unstandardized Bayesian parameter estimates. Standardized estimates for significant paths are graphically displayed in Fig 2c.

Table 3

DAN_{ALFF} is negatively associated with higher affective instability

Predictor	$t_{unconditional}$	$p_{unconditional}$	$t_{conditional}$	$p_{conditional}$	$\overline{R^2}_{dom}$
$Impulsivity_{BPQ}$	-2.64	0.010^{**}	-1.07	0.291	0.009
$Affective\ Instability_{BPQ}$	**-3.97**	**0.002^{**}**	**-2.87**	**0.005^{**}**	**0.035**
$Abandonment_{BPQ}$	-2.38	0.020^{*}	-0.04	0.970	0.009
$Relationships_{BPQ}$	-2.68	0.009^{**}	-0.24	0.815	0.017
$Self\text{-}Image_{BPQ}$	-2.13	0.036^{*}	0.29	0.771	0.020
$Suicide/Self\text{-}Mutilation_{BPQ}$	-2.04	0.045^{*}	1.32	0.192	0.012
$Emptiness_{BPQ}$	-2.08	0.041^{*}	-0.08	0.936	0.006
$Intense\ Anger_{BPQ}$	-1.80	$0.075^{\dagger}$	0.68	0.500	0.004
$Quasi\text{-}Psychotic\ States_{BPQ}$	-1.15	0.256	0.63	0.532	0.010
$\overline{ALFF}$	11.75	$<0.001^{***}$	11.30	$<0.001^{***}$	0.590

Note. Predictor column reflects BPQ subscales that were used to predict DAN_{ALFF}. $\overline{ALFF}$ represents a nuisance covariate calculated as a subject-specific mean of regional ALFF values. $t_{unconditional}$ and $p_{unconditional}$ reflect test statistic and p-value for separately fit linear models for each BPQ subscale, where $t_{conditional}$ and $p_{conditional}$ reflect test statistic and p-value for parameters of a joint multiple regression, where subscales compete to explain variance in DAN_{ALFF} (see *Associations with BPD Symptom Domains* in Methods). $\overline{R^2}_{dom}$ represents the average change in model R^2 when entering this symptom scale into nested sub-models in a dominance analysis signaling the relative importance of heightened affective instability in predicting lower DAN_{ALFF} compared to other BPD symptom domains.